Assessment of a flexible solar hybrid thermal and electrical prototype

Brice Lecœuvre, Ghjuvan Antone Faggianelli, Jean-Louis Canaletti, Christian Cristofari

Assessment of a flexible solar hybrid thermal and electrical prototype

Brice Lecœuvre[a,*], Ghjuvan Antone Faggianelli[a], Jean-Louis Canaletti[a], Christian Cristofari[a]

[a] *Université de Corse - CNRS UMR 6134 SPE, Ajaccio, France*

Abstract

This paper presents a study of a new system called Système Réfléchissant à Lames Orientables (Orientable Blades Reflective System) (SRLO). This solar hybrid concentrated system is able to produce both thermal and electrical energy. Following the technological advances of recent years, it appears as the outcome of several prototypes improved over time. SRLO can now be considered as a flexible distributed generation system which can be integrated into a microgrid.

First, we present the evolution of the system over time and its operation. Then, we focus on the astronomical parameters representing the position of the sun and the specific trigonometric calculations of reflections and shadows. They make it possible to calculate the energy optimum, to operate the control- command and to define the operating profiles. These parameters are also used to obtain the optimal position of the receiver considering the shadow of the reflecting structure. Finally, this study allows the estimation of the concentration rate of the system at any time as well as the solar energy received by the PV modules.

Keywords: Solar concentrating system, Linear Fresnel Reflector (LFR), hybrid system, electrical/thermal energy

1. Introduction

Most countries of the world aim to develop Renewable Energy Sources (RES). However, intermittent sources such as wind turbines and photovoltaic power stations may have a negative impact on electrical grid without a suitable management, in particular for island areas. In the last decades, their

*Corresponding Author
Email address: lecoeuvre_b@univ-corse.fr (Brice Lecœuvre)

increase have brought new challenges in terms of energy storage and control. In this context, the development of microgrids including Distributed Energy Resources (DER) appear to be a promising solution to build a more reliable grid while increasing the share of RES. The key technologies required to achieve successful deployment of microgrids include advanced components as well as advanced control strategies. As a locally controlled system, a microgrid should be able to ensure continuous supply of electrical and possibly thermal loads. It is thus especially important to develop easily controlled Distributed Generation (DG) which bring more flexibility and reliability.

Combined Heat and Power (CHP) is a mature and well-known process allowing simultaneous generation of electricity and useful heating. Advantages and disadvantages of CHP systems have been widely described in literature [1]. It should be noted that heat is generally lower-quality energy than electricity and both heating and electricity demand must remain fairly consistent. Also, CHP systems do not allow modulation of one source with respect to the other. They are thus not suitable for all sites and must be seen more as a mean of extending energy rather than two actual energy sources.

An other way to produce both electricity and useful heating is to use PhotoVoltaic-Thermal (PVT) solar systems [2]. A significant amount of work has been carried out on these systems since 1970 and most recent ones such as the Hybrid Electric And Thermal Solar (HEATS) aim to reach an efficiency greater than 35% [3]. Performances can also be increased with the use of Concentrated PhotoVoltaic Thermal (CPVT) [4]. The main advantage of this technology lies in the possibility to reach higher temperature while increasing efficiency of the photovoltaic side [5]. However, as for standard CHP systems, the production of useful heating is still directly related to the electricity one, which may be a concern according to the needs.

Other than these types of technologies, real hybrid systems with fully adjustable production of electrical and thermal energy are not described in literature. For specific case studies, highly variable needs of heat and electricity can be observed over the time. Energy storage is one of the key to overcome this issue but is no more suitable if there is no need of one energy source over a long period.

In the framework of the research project PAGLIA ORBA, the laboratory SPE (University of Corsica, France) aims to test and characterise components of a solar microgrid at the scale of a village or a neighborhood. This paper focuses on a prototype of an easily controlled DG system which can produce both electrical and thermal energy simultaneously or individually. The last

prototype of the so-called SRLO system is a concentrating hybrid solar power system composed of several reversible and controllable blades:

- One side of each blade is a mirror which concentrates solar radiation on a fixed receiver.
- The other side integrates photovoltaic modules.

Since the first publication produced in 1980 by Peri [6], this system has known a number of evolutions.

1.1. First prototype

At the time, the invention of the first prototype, called *linear concentration solar collector*, responds to a specific demand: to produce thermal energy at medium temperature. This solar concentrating system, presented in figure 1, belongs to the category of Linear Fresnel Reflective (LFR). Most LFR are positioned facing the sky [7] [8]. Indeed, the structure supporting the mirrors is parallel to the ground and the axis of rotation of the mirrors is north-south, in order to keep track of the azimuth. This prototype does not exactly follow this pattern: its structure is tilted at 60° to the south, and the axis of the mirrors is east/west. This type of system is more adapted to the location studied with a latitude of 42.30°.

The first problem that arises for the conversion of solar radiation is the choice of the thermal converter. Several solutions are depending on the type of use, from simple fixed plane collector, with a simple greenhouse effect, to parabolic system equipped with a structure to follow the sun. The choice of collector depends on the desired temperature level. The operating temperature of the prototype was $140°C$. To meet this requirement in steady state, fixed plan collector even equipped with elaborate anti-loss devices can no longer compete with solar concentrating systems. Conversely, high flow rate collectors lose their interest when the level of requested temperature is low; these facilities are too complex and expensive to use at low temperatures. At the time, vacuum collectors were not a option as their commercialisation was only beginning to emerge [9] [10].

Unlike conventional parabolic and cylindro-parabolic systems, the receiver and the reflective structure are completely independent from a mechanical point of view. The receiver is very elongated, facing north, and placed so that its main axis is oriented east/west. The entire receiver is placed at a certain height to optimise the received radiation. The reflective

structure supports a number of plane mirrors, mobile around the east/west axis.

Several works have been done by Pasquetti, allowing the validation of a first numerical model, realised with punch cards [11] [12]. A numerical model study has been carried out to give a first insight of the production of such device. This study was made for a latitude for 43.30° corresponding to the location of Marseille (France) with an operating temperature of $140°C$. A mean efficiency $\eta_{receiver}$ of 0.59 has been obtained.

Even if the production of thermal energy remains "moderate" (low temperature) compared to a parabolic system (high temperature), this prototype has many advantages:

- easy implementation, through the simplicity of the system;
- easy maintenance, through this same simplicity;
- low cost price, through the use of a structure of rustic concentration and simplified tracking (single axis);
- interesting temperature level for number of applications (between $120°C$ and $160°C$);
- fixed receiver near the ground level and therefore easily accessible;
- good protection of the mirrors against dirt, through the possibility of orienting them towards the ground in periods of non-use and towards the sky during periods of rain;
- very high wind resistance of the reflective structure;
- functional safety facilitated by the possibility of defocusing the mirrors.

1.2. Second prototype

In the years 1985, a second prototype is conceived on the site of University of Corsica (Ajaccio, France) thanks to Pr. Georges Peri. It is also composed of a longitudinal structure oriented east/west. This supports the moving axes of four units of sixteen aluminium blades and composed of a reflective surface. The axes of each line are coupled at the end of the structure by pulleys interconnected by a steel cable.

This system makes it possible, with a simple movement, to obtain an equal angular variation for all the mirrors and to transform it into a linear variation. This second version is also a system that is positioned manually, with a handle that allows linear movement of the cable. In addition, the dimensions of the structure have been changed. The structure is inclined at 60° to the horizontal, with a height of 2 m and a length of 10 m. it is composed of sixteen blades measuring 10 cm × 24 cm.

1.3. Third prototype

In 1990, a third prototype is realised. The main innovation is the automation of the blades positioning, so that the focus of solar radiation is ensured throughout the year. To do this, the design of a servo of the blades position is essential. In the study done by Canaletti [13], two types of techniques are used. A first, based on optoelectronic technique with cells sensitive to solar radiation and an electronic control. A second, using computer which, with the help of data on the trajectory of the sun, corrects the angular position of the mirrors. Finally, a control-command acts on the hydraulic actuator which allows placing all the mirrors at the same time to insure the focusing of solar radiation on the receiver.

Now, the system moves these blades automatically. However, it still has drawbacks :

- several elements require a source of electrical power to function as the pump, the three-way valves, the hydraulic actuator and the control-command;
- the enslavement of mirrors works in *on/off* mode.
- the pump has a constant flow.

When the set-point temperature is exceeded, the action of the hydraulic actuator defocuses all the mirrors. The hysteresis comparator is difficult to set. In fact, all the mirrors move at the same time and cause large variations of power.

This paper thus focuses on the description of a new prototype, which main purpose is to mitigate these drawbacks. First, we provide a general description of the system, to highlight the main evolutions. Then we focus on the solar and geometric parameters required to control the system. To

conclude, main results are discussed and some recommendations and outlooks are proposed.

2. New prototype

2.1. General description

Previously, this system could only produce thermal energy. The new prototype can still produce thermal energy (figure 2), with the concentration of solar radiation, but can also produce electrical energy (figure 3) through the modules positioned on the back. Such system can now also be seen as a DG of a microgrid.

It has 64 blades with a length of 2.42 m and a width of 10 cm. Blades are composed of a reflective surface on one side and on the other side of a surface integrating photovoltaic modules. Four polycrystalline modules are installed per blade, with a length of 600 mm and a width of 100 mm. The real dimensions of the module surface are 538 mm $\times$ 77 mm, with a peak power of 5 W per module. The total area of the module is 10.7 m^2, resulting in a total peak power of 1280 W.

For the solar radiation concentration part, the blades are covered by mirrors made of aluminium foil, which is placed under a glass pane to ensure its protection. The aim is to produce thermal energy at a constant temperature as often as possible. The enslavement of each blade is now performed independently. To do this, gear motors are placed at the end of each blade. Independent control of mirrors can modulate the concentration and thus enslaves the temperature level. If a mirror is defocused, it can be directed to incident radiation to produce electrical energy. This energy is then stored in batteries.

This prototype can therefore operate in three different modes:

- thermal mode,
- electrical mode,
- thermal/electrical mode.

The electrical mode ensures the operation of the system and can also supply power to an external load.

The hydraulic loop has been also improved. It is first equipped with six three-way valves to use the four receivers in five different modes. The

configuration of the receivers may be in serial mode, in parallel mode or in intermediate modes. To improve the temperature level, the conventional pump has been replaced by two solar pumps with variable flow. They operate in DC current and have a Maximum Power Point Tracking (MPPT). The control-command can now operate in real time. It adapts the operation of the primary loop according to the incident radiation and the set temperature. Previously, the conventional greenhouse emitter was not suitable for this type of system because the glass heated quickly when all the mirrors were focused on the solar radiation. With all these improvements, three types of servo are possible:

- modulation of the concentration by servocontrolling each mirror line;
- modulation of the flow rate by servocontrol of the variable flow solar pumps; modulation of the concentration coupled with the modulation of the flow rate.
- modulation of receiver configuration.

The system, shown in the figure 4, is now able to produce thermal energy respecting a set temperature, but also to produce electrical energy for its autonomy and external load. The nominal and maximum power of the control is respectively 87 and 165 W. We consider that during a day, the system operates with maximum consumption for a duration of 4 hours and the remaining time at its nominal consumption. This results in a daily consumption of 2.4 kWh.

2.2. Receivers

The solar radiation reflected by the mirrors is focused on four linear receivers. They are equipped with black absorbers to limit the reflection of solar radiation increasing its efficiency. The absorbers are made of two aluminium plates. Between these two plates, a copper tube with an external diameter of 10 mm is positioned. All these elements are welded together by ultrasound to ensure high thermal contact. The absorber is positioned on the front of each receiver. An insulation of 5 cm surrounds the absorber. Here are the values characterising the receiver:

- the dimensions of each receiver are $L_{receiver} = 205\ cm$ and $l_{receiver} = 25\ cm$;

- the aluminum casing has an absorption value of $\alpha_{alu} = 0.90$;
- the dimensions of the glass of the absorber are $L_{glass} = 195\ cm$ and $l_{glass} = 15\ cm$;
- the glass has an absorption value of $\alpha_{glass} = 0.055$ and a transmittance value of $\tau_{glass} = 0.866$;
- the dimensions of each absorber are $L_{abs} = 195\ cm$ and $l_{abs} = 15\ cm$;
- the total area of absorbers is $S_{abs} = 1.17\ cm^2$
- the absorber has an absorption value of $\alpha_{abs} = 0.95$;
- this results in a geometric concentration corresponding to 13.2, by establishing the ratio between the total surface of the mirrors and the total surface of the absorbers;
- the height of the receiver (between the ground and the middle of the absorber) is 74 cm.
- the distance between the reflective surface and the receiver is 1 m. This distance can be changed, but then the precision of the motor that focuses the solar radiation will have to be changed as well. Currently the rotation of 1 degree of the farthest mirror causes a *spot* shift on the receiver of more than 10 cm.

A three-dimensional model of one of the receivers is shown in figure 5.

2.3. Hydraulic circuit

The hydraulic circuit (figure 6) allows the circulation of the heat transfer fluid. It consists mainly of copper tubes with a diameter of 12 mm. The thermal insulation of these tubes is ensured by a heat-insulated sheath of 10 mm thickness, made of synthetic rubber-based foam (elastomer). This hydraulic circuit consists of:

- a black tank called the discharge tank, made of steel (2 mm thick), with a storage capacity of 300 liters; it simulates a thermal load;
- an insulated Domestic Hot Water (DHW) tank of 300 liters, for storing water at a temperature from $60°C$ to $70°C$;

- seven three-way solenoid valves, which make it possible to shunt the DHW and allow different configurations of the receivers (figure 7);
- two variable speed pumps for modulating the flow of the fluid.

In fact, the purpose of the system is to respond to a thermal load; if the supply of this load is guaranteed, then it can store the thermal energy in the DHW tank.

3. Solar and geometric parameters of the system

3.1. Angular height of the sun in the north/south plane

To know the angular elevation of the sun seen from this plane, it is necessary to realise its orthogonal projection. Let h_p be the projection of the angular height of the sun in the plane of the structure that we call projected angular height:

$$\tan(h_p) = \frac{\tan(h)}{\cos(\Psi - \gamma)} \tag{1}$$

Due to boundary conditions ($\Psi = 90°$) the equation is:

$$\tan\left(\frac{\pi}{2} - h_p\right) = \frac{\cos(\Psi - \gamma)}{\tan(h)} \tag{2}$$

3.2. Solar deviation

To find the solar deviation from the plane, as shown in figure 8, it is necessary to calculate the projected solar deviation angle Ψ_p formed by the incident radiation and its projection in the plane. We get the relation:

$$\cos(\Psi_p) = \cos(h)\ \sin(\Psi - \gamma) \tag{3}$$

3.3. Angle of inclination of mirrors

The enslavement of the positioning of the mirrors to ensure a focus of the solar radiation is based on the calculation of the angles of inclination of the mirrors. The parameters used to obtain these values are the date, the time and the coordinates of the place. The use of these parameters requires knowledge of the geometry of the system:

- D_N: the projected distance on the horizontal plane between each

$$D_N = D + \cos(\beta)\, N\, X \tag{4}$$

- H_{2_N}: the height of each mirror N, whose expression is:

$$H_{2_N} = \sin(\beta)\, N\, X \tag{5}$$

That is, h_{m_N} the difference in angular height between each mirror N and the receivers:

$$h_{m_N} = \arctan\left(\frac{H_1 - H_{2_N}}{D_N}\right) \tag{6}$$

If h_p is the projected angular elevation of the sun and h_{m_N} the difference in angular height of each mirror N, then, by Descartes' relation, we obtain, for each mirror, the angle of incidence projected on the horizontal plane including the normal to the mirror, Θ_{p_N}:

$$\Theta_{p_N} = \frac{h_p - h_{m_N}}{2} \tag{7}$$

So the inclination β_{1_N} of each mirror N with respect to the vertical is expressed:

$$\begin{aligned} \beta_{1_N} &= \Theta_{p_N} + h_{m_N} \\ \beta_{1_N} &= \frac{h_p + h_{m_N}}{2} \end{aligned} \tag{8}$$

The use of these angles of inclination for each mirror allows the focusing of solar radiation on the receivers.

3.4. Width of the spot on the receiver

The width of the *spot* varies only according to the angles of inclination of the mirror and the receiver:

$$l_{a_N} = l_{mirror} \frac{cos(\beta_{1_N} - h_p)}{cos(\beta_2 - h_p)} \tag{9}$$

3.5. Angle of movement

The angle called *angle of movement* represents the angle swept by a reflected ray to traverse the remaining distance between the edge of the *spot* and the edge of the receiver. The calculation of this parameter makes it possible to optimise the consumption of the system. In fact, we will know the actual time before which the *spot* must leave the receiver and therefore the time interval between two readjustments. The parameters (figure 9) useful for obtaining this time interval are described in the appendix.

3.6. Exit time from the edge of the spot

The angle swept through a reflected ray to traverse the receiver is now known. It is now necessary to calculate the exit time of the *spot*.

- h_p and ω: respectively the projected angular height of the sun and the hour angle at time t_1

- ω_{S_N}: the new hour angle, for h_p corrected by hc_{1_N} or hc_{2_N} depending on the case, knowing that:

$$\cos(\Psi) = \frac{\sin(h)\ \sin(\phi) - \sin(\delta)}{\cos(h)\ \cos(\phi)} \tag{10}$$

$$\tan(h_p) = \frac{\tan\left(h\right)}{\cos(\Psi - \gamma)} \tag{11}$$

We get h based on h_p :

$$\begin{aligned} \sin(h) &= \frac{\sin(\delta)\ \tan(h_p)}{\sin(\phi)\ \tan(h_p) - \cos(\phi)} \\ &= \frac{\sin(\delta)}{\sin(\phi) - \cos(\phi)\ \tan\left(\frac{\pi}{2} - h_p\right)} \end{aligned} \tag{12}$$

Knowing also that:

$$\begin{aligned} \sin(h) = &\cos(\delta)\ \cos(\phi)\ \cos(\omega) \\ &+ \sin(\delta)\ \sin(\phi) \end{aligned} \tag{13}$$

We get ω depending h:

$$\cos(\omega) = \frac{\sin(h) - \sin(\delta)\ \sin(\phi)}{\cos(\delta)\ \cos(\phi)} \tag{14}$$

Depending on the time of year, this time interval is obtained differently:

- First case: between the equinox of spring and autumn, h_p increases in the afternoon, so we correct h_p by adding hc_{1_N}. We calculate the corresponding hour angle ω_{S_N}, then we deduce the corresponding time T:

$$T_{N_s} = \frac{|\omega - \omega_{S_N}|}{0.2618} \tag{15}$$

- Second case: between the equinox of autumn and spring, h_p decreases in the afternoon, so we correct h_p by subtracting hc_{1_N}. We calculate the corresponding hour angle ω_{S_N}, then we deduce the corresponding time T, as in the first case.

- Third case : to obtain the exit time of the *spot* in the morning between the equinox of spring and autumn, it is necessary to calculate the angle of the mirrors at solar noon, because at this moment their movement is reversed:

  - if h_p corrected by hc_{2_N} is smaller than the angle at solar noon, we calculate as before ω_{S_N} et T_N;
  - if h_p corrected by hc_{2_N} is larger than the solar angle at noon, the time elapsed until solar noon is calculated:

$$T_{1_N} = \frac{|\omega|}{0.2618} \tag{16}$$

Then we calculate ω_{S_N} corresponding to h_p corrected, this time, by hc_{1_N} (since the movement is reversed) and of the angle travelled until noon solar. We therefore deduce the time T_{2_N}:

$$T_{2_N} = \frac{|\omega_{S_N}|}{0.2618} \tag{17}$$

The exit time is:

$$T_N = T_{1_N} + T_{2_N} \tag{18}$$

- Fourth case: to obtain the exit time of the *spot* in the morning between the equinox of autumn and spring, we apply the same reasoning as in the third case.

All these equations are essential for the control-command.

4. Receiver height optimisation

The optimisation of the height of the receivers is an essential step (figure 10) to obtain maximum energy. To do this, an energy study to know the power arriving at the receivers, integrated throughout the year, has been conducted. This work has three stages. Beforehand, a first step is to calculate the energy received by the absorber of the receiver without taking into account the solar deviation. A second step is performed, with the same calculation, but considering also the solar deviation. Finally, the shading effect of by the receivers on the reflective structure is considered. This makes it possible to quantify the real energy arriving on the absorber. This approach allows the calculation of the energy lost by the deviation and the impact of the shadow caused by the receivers.

4.1. Assumption

The optimum height of the receiver is obtained when the angle of incidence is the lowest for all the mirrors, for all the days of the year. The first set of assumptions are:

- no energy losses due to solar deviation;
- purely geometrical consideration;
- use of the theoretical value of extraterrestrial radiation (we do not consider losses due to cloudiness, rain, pollution, etc.);
- all the energy received by the mirrors is concentrated on the absorbers of the receivers.

The calculation is the sum of the resulting powers of the sixteen mirrors integrated throughout the year. We know that :

- the power at a given moment for each mirror N, corresponds to the equation:

$$P_{1_N} = S_{mirror}\, I_0\, \cos(\Theta_{p_n}) \tag{19}$$

  with S_{mir} corresponding to the surface of a line of mirrors and $I_0 =$ 1 367 W.

- to obtain the annual energy, one needs to integrate the power on each day of the year; we choose the minute as time step.

Then, with the same assumptions as before, we integrate the energy loss due to solar deviation. We must therefore calculate the new lengths of each mirror N:

$$L_{1_N} = D_N\, \tan(\Psi - \gamma) \tag{20}$$

L_{1_N} is then evaluated to know the real energy that arrives on the absorbers of the receivers. In fact, the system is equipped with four concentration modules that are assembled together; the system therefore has spaces between the modules. These spaces are taken into consideration as well as the exact position of the focus of each mirror.

Finally, we quantify the energy loss due to the shadowing effect of the receiver, on the structure.

For each geometric parameter of the system, several calculations are established and the choice of equations will vary according to the time, day and season. A condition set will select the proper equation depending on the position of the sun and that for each parameter.

4.2. Results and discussions

The figure 11 shows that the energy received, without taking into account the solar deviation, is important (46.4 $MWh.yr^{-1}$). The effect of solar deviation induces an energy loss of 20.9 %. The energy received is then 36.7 $MWh.yr^{-1}$. The third assumptions induces an energy loss of 29.4 % compared to the first, with an energy production of 34.6 $MWh.yr^{-1}$. The

optimal heights of the solar receiver for the three studies, are respectively 234 cm, 168 cm and 143 cm (figure 12).

In all three cases (figure 13), the largest energy production is obtained around the equinoxes. The height of the receiver has a lot of influence on the difference in production in winter and summer. Indeed, if we decrease this height, the production will be higher in winter and lower in summer.

In order to obtain an annual energy maximum, a receiver height between 70 cm and 150 cm with a receiver-structure distance of 1 m is possible. In this range, the energy loss against the optimal value is less than 1%.

We recommend to minimize the receiver height (74 cm for our prototype), as this bring a lower cost of materials (shorter length), a less complicated installation to realise and a less difficult maintenance to perform.

Finally, the energy from the reflective surface is much higher than the energy received by the absorbers. The losses are mainly due to the solar deviation and the spacing between the absorbers. To recover this lost energy, it would be first necessary to remove the space between the absorbers and then to reduce the azimuth effect. For this, three ways to proceed. A first is to increase the length of the mirrors knowing that the energy from the reflective surface will be further increased relative to the energy received by the absorbers (higher geometric concentration). Reflectors could also be positioned to recover lost energy. A last method would be to make the absorbers mobile and position them according to the solar deviation. The latter is not very realistic even if it is technically possible.

5. Concentration rate

When considering solar concentration, we often refer to the geometric concentration factor. Indeed, this factor is still applicable for concentrating systems that follow the sun on two axes. For concentrating systems that follow the sun on a single axis, such as the one studied in this paper, this concentration factor is not the same:

$$\eta_{SRLO} = \frac{S_{mir_{tot}}}{S_{abs_{tot}}} \tag{21}$$

This factor is maximum at solar-noon for a south-facing system. In order to know the actual concentration rate, the parameter S must represent the surface of the *spot* reflected by the mirrors of the system that arrives on the absorber.

The figure 14 illustrates the actual concentration rate during a day of equinox, summer solstice and winter solstice. As we have chosen a low height of receiver, 74 cm, the concentration rate is higher during winter.

The figure 15 shows this same concentration rate as a function of azimuth angle. For a single axis system, the concentration rate only exists when the sun is in front of the system. As the SRLO is not perfectly south-facing, the corresponding azimuth angles at the equinox are not exactly $\pm$ 90°.

It can be seen in figures 14 and 15 that the actual concentration rate is always lower than the geometric concentration factor of 13.2. This shows that this factor should not be considered for a single axis system as it tends to overestimate the solar radiation received by the mirrors. If the length of the reflective surface was identical to the length of the absorbers, this factor should be reached at solar-noon for a south-facing system. For the SRLO, this factor is never reached as the length of the reflective surface is actually greater than the length of the absorbers.

These figures also show that the geometry of SRLO is optimised for winter. For the same period, it can be seen that the shadow of the receiver has important influence on the concentration rate. The longest period to produce thermal energy is during the equinox. The actual concentration rate will allow us to improve the operating profiles.

6. Conclusion

SRLO is a hybrid system that can produce both thermal energy and electrical energy. It consists in a fixed structure supporting sixteen movable blades, which can either concentrate solar radiation on a fixed receiver with mirrors or produce electricity with photovoltaic modules.

The system described in this paper is the outcome of several prototypes improved over time. In this last version, PV modules have been added to cover self-supply of the system and potential external loads, with the possibility of storing electricity in batteries. Also, all blades can now move independently, thanks to geared motors. It is then possible to defocus each mirror individually, in order to modulate the concentration and thus to enslave the temperature level. In parallel, PV modules can be oriented towards direct or diffuse radiation depending on the weather.

Considering the hydraulic system, the primary loop has been improved with the addition of six three-way valves, allowing the use of four receivers

in five different modes. From serial mode to parallel mode, the control-command can, in real time, adapt the operation of the primary loop according to the incident radiation, the stored heat and the power of the load. To improve the temperature level, two solar pumps can now regulate the flow of the hydraulic circuit. Servo-control of the outlet temperature can thus be achieved in three different ways: variation of the flow of the hydraulic loop, action on the concentration rate and action on the receiver configurations.

The study of the solar parameters made it possible to know at any moment the solar radiation, with or without reflection, on all the elements of the system. For this purpose, system-specific trigonometric calculations of reflection and shadows have been provided, allowing the calculation of the energy optimum. These parameters have been used to determine the optimal position of the receiver with respect to the structure. The receiver should be positioned at a distance of one meter in front of the structure and at a height of 74 cm. The remaining losses are mainly due to the effect of the solar deviation and the fact that the absorbers are spaced apart. To limit these losses, it would be first necessary to remove the space between the absorbers, and then to reduce the azimuth effect by increasing the length of the mirrors or adding reflectors to recover lost energy.

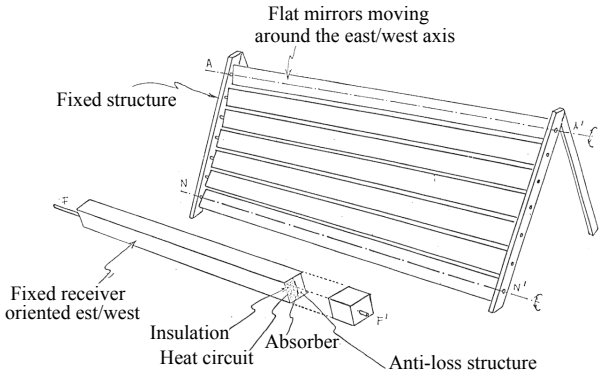

Figure 1: First diagram of the prototype (1981)

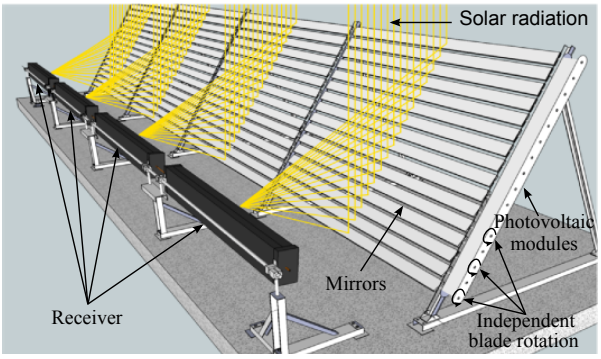

Figure 2: Three-dimensional modelling: thermal part

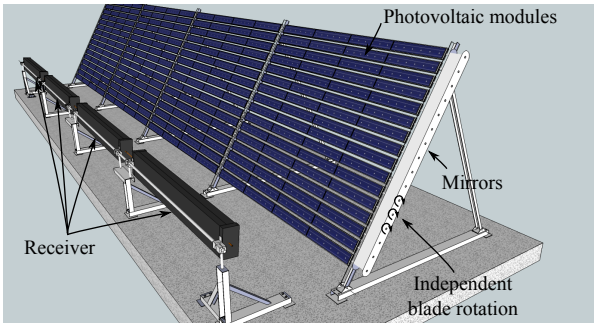

Figure 3: Three-dimensional modelling: electrical part

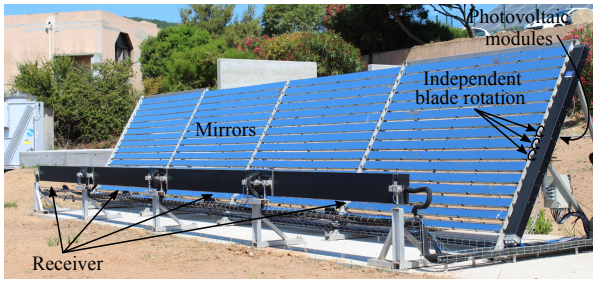

Figure 4: Picture of the solar concentration system

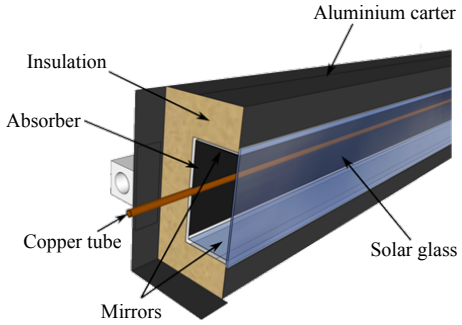

Figure 5: Three-dimensional modelling: receiver

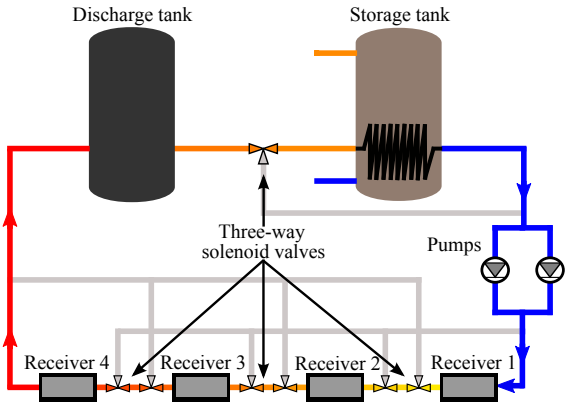

Figure 6: Hydraulic circuit

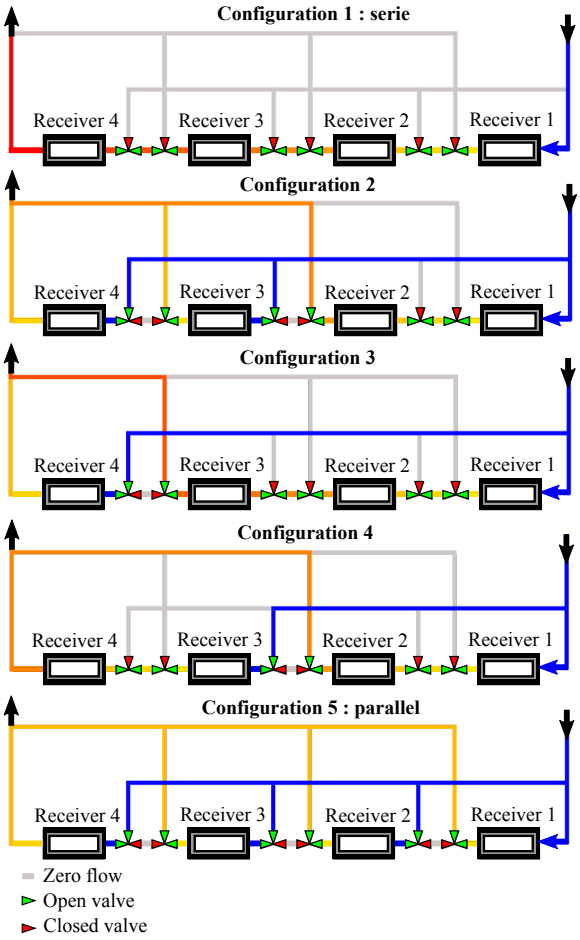

Figure 7: Modular receiver: different configurations possible

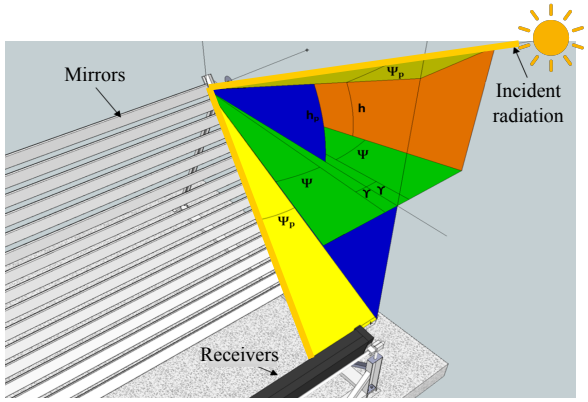

Figure 8: Specific parameters solar system

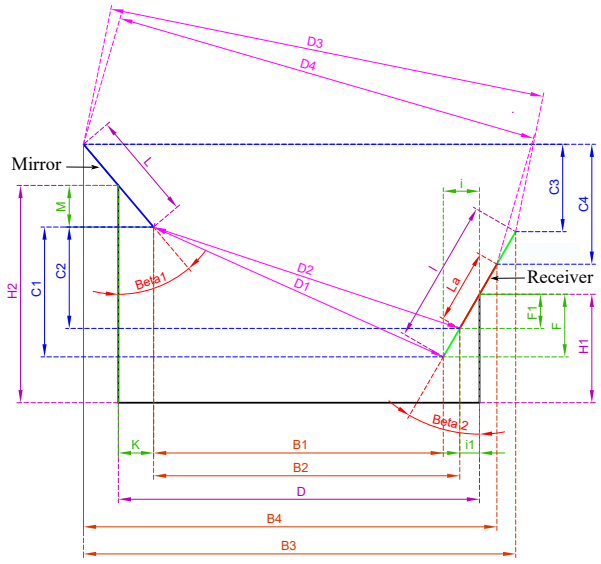

Figure 9: Geometric parameters of the system

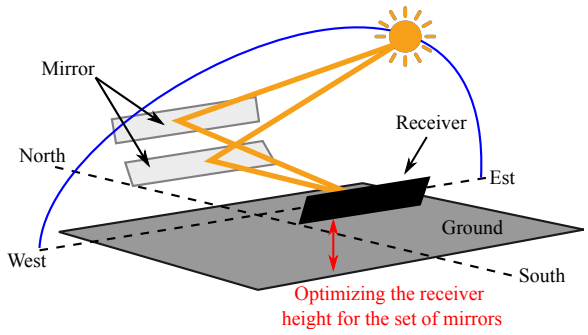

Figure 10: Receiver height optimisation

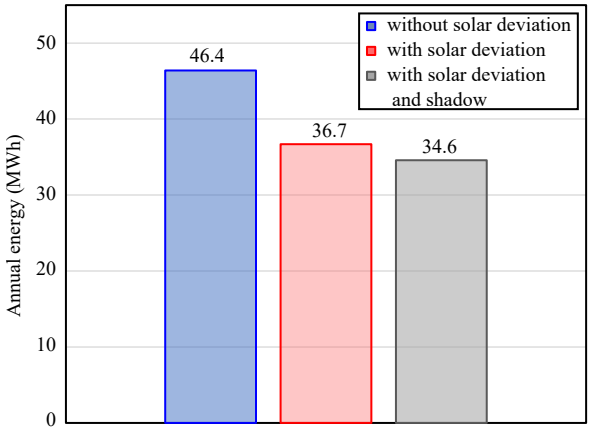

Figure 11: Annual energy received

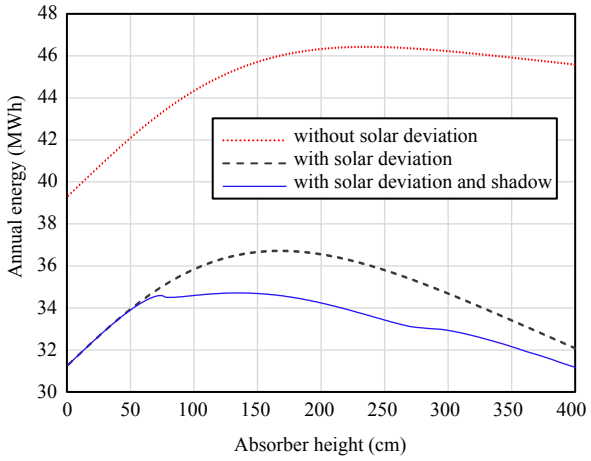

Figure 12: Annual energy received depending on the height of the absorber

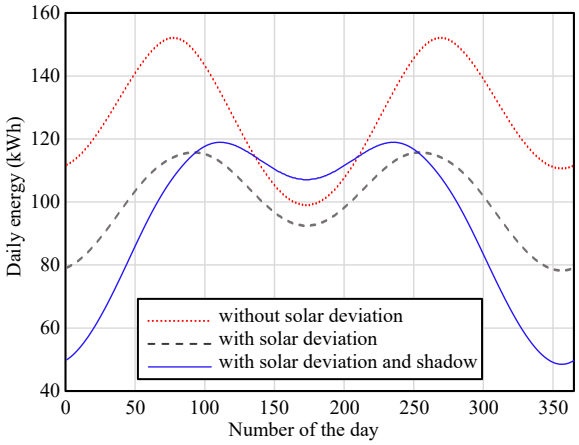

Figure 13: Daily energy

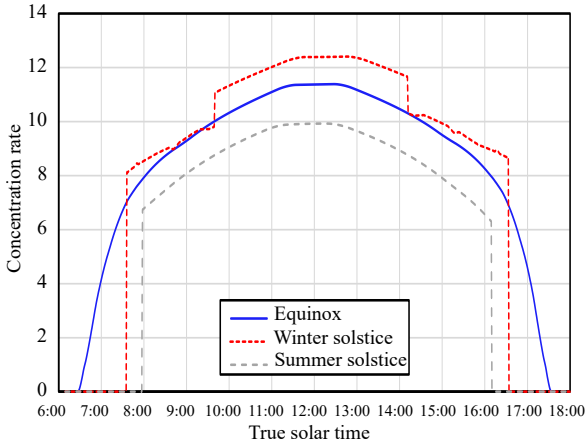

Figure 14: Concentration rate as a function of time

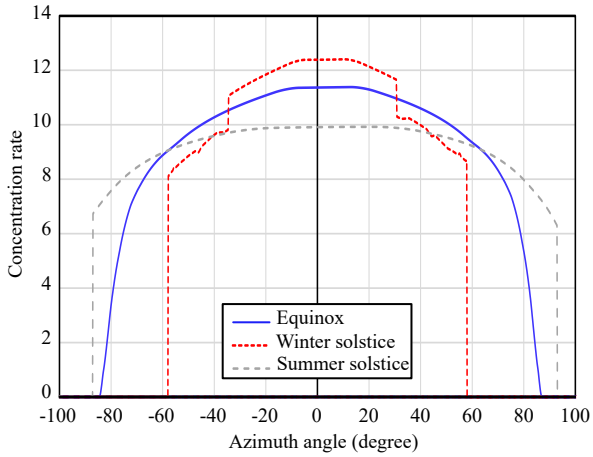

Figure 15: Concentration rate as a function of azimuth angle

Appendix A. Geometric parameters of the system

$$K_N = \frac{L\ \sin(\beta_{1_N})}{2} \tag{A.1}$$

$$M_N = \frac{L\ \cos(\beta_{1_N})}{2} \tag{A.2}$$

$$I = \frac{l\ \sin(\beta_2)}{2} \tag{A.3}$$

$$F = \frac{l\ \cos(\beta_2)}{2} \tag{A.4}$$

$$I_{1_N} = \frac{L_{A_N}\ \sin(\beta_2)}{2} \tag{A.5}$$

$$F_{1_N} = \frac{L_{A_N}\ \cos(\beta_2)}{2} \tag{A.6}$$

$$B_{1_N} = D_N - I - M_N \tag{A.7}$$

$$B_{2_N} = D_N - I_{1_N} - M_N \tag{A.8}$$

$$B_{3_N} = D_N + I + M_N \tag{A.9}$$

$$B_{4_N} = D_N + I_{1_N} + M_N \tag{A.10}$$

$$C_{1_N} = (H_1 - F) - (H_{2_N} - K_N) \tag{A.11}$$

$$C_{2_N} = (H_1 - F_{1_N}) - (H_{2_N} - K_N) \tag{A.12}$$

$$C_{3_N} = (H_1 + F) - (H_{2_N} + K_N) \tag{A.13}$$

$$C_{4_N} = (H_1 + F_{1_N}) - (H_{2_N} + K_N) \tag{A.14}$$

$$D_{1_N} = \sqrt{\left({B_{1_N}}^2 + {C_{1_N}}^2\right)} \tag{A.15}$$

$$D_{2_N} = \sqrt{\left({B_{2_N}}^2 + {C_{2_N}}^2\right)} \tag{A.16}$$

$$D_{3_N} = \sqrt{\left({B_{3_N}}^2 + {C_{3_N}}^2\right)} \tag{A.17}$$

$$D_{4_N} = \sqrt{\left({B_{4_N}}^2 + {C_{4_N}}^2\right)} \tag{A.18}$$

$$\cos(hc_{1_N}) = \frac{{D_{1_N}}^2 + {D_{2_N}}^2 - \left(\frac{1}{2} - \frac{L_{A_N}}{2}\right)^2}{2\, D_{1_N}\, D_{2_N}} \tag{A.19}$$

$$\cos(hc_{2_N}) = \frac{{D_{3_N}}^2 + {D_{4_N}}^2 - \left(\frac{1}{2} - \frac{L_{A_N}}{2}\right)^2}{2\, D_{3_N}\, D_{4_N}} \tag{A.20}$$

Nomenclature

α_{abs}	Absorbance of the absorber	[ ]
α_{alu}	Absorbance of the aluminum casing	[ ]
α_{glass}	Absorbance of the glass	[ ]
β	Angle of inclination of the structure in relation to the horizontal	[rad]
β_{1_N}	Angle of inclination of each mirror N with respect to the vertical	[rad]
β_2	Angle of inclination of the receivers with respect to the vertical	[rad]
δ	Solar declination	[rad]
$\eta_{receiver}$	Receiver efficiency	[ ]
η_{SRLO}	Concentration rate	[ ]
γ	Angle of deviation of the south and the normal of the inclined surface projected on the ground	[rad]
ω	Hour angle	[rad]
ω_{S_N}	Corrected hour angle of hc_{1_n} ou de hc_{2_n} (which is therefore a function of each mirror N)	[rad]
ϕ	Latitude	[rad]
Ψ	Azimuth angle	[rad]
Ψ_p	Solar deviation	[rad]
τ_{glass}	Transmittance of the glass	[ ]
Θ_{p_N}	Angle of incidence projected on the horizontal plane including the normal to the mirror N	[rad]
B_{1_N}	Distance projected on the horizontal plane from the lower end of each mirror N to the lower end of the receiver	[cm]
B_{2_N}	Distance projected on the horizontal plane from the lower end of each mirror N to the lower end of the *spot*	[cm]

B_{3_N}	Distance projected on the horizontal plane from the upper end of each mirror N to the upper end of the receiver	[cm]
B_{4_N}	Ddistance projected on the horizontal plane from the upper end of each mirror N to the upper end of the *spot*	[cm]
C_{1_N}	Difference height between the lower end of each mirror N and the lower end of the receiver	[cm]
C_{2_N}	Difference height between the lower end of each mirror N and the lower end of the *spot*	[cm]
C_{3_N}	Difference height between the upper end of each mirror N and the upper end of the receiver	[cm]
C_{4_N}	Difference height between the upper end of each mirror N and the upper end of the *spot*	[cm]
D	Distance projected horizontally between the structure and the receivers	[cm]
D_{1_N}	Distance between the lower end of each mirror N and the lower end of the receiver	[cm]
D_{2_N}	Distance between the lower end of each mirror N and the lower end of the *spot*	[cm]
D_{3_N}	Distance between the upper end of each mirror N and the upper end of the receiver	[cm]
D_{4_N}	Distance between the upper end of each mirror N and the upper end of the *spot*	[cm]
D_N	Projected distance on the horizontal plane between each mirror N	[cm]
F	Projection of the half-width of the receiver on the vertical	[cm]
F_{1_N}	Projection of the half-width of the *spot* on the vertical according to each mirror: N	[cm]
h	Angular height of the sun	[rad]

533	H_1	Receiver height	[cm]
534	H_{2_N}	Height of each mirror N	[cm]
535	h_{m_N}	Difference in angular height between each mirror N and the receivers	[rad]
537	h_p	Angular height of the sun in the north-south plan	[rad]
538	hc_{1_N}	Angle scanned by a ray reflected from the top end of each mirror N to traverse the distance between the top edge of the task and receivers	[cm]
541	hc_{2_N}	Angle scanned by a ray reflected from the lower end of each mirror N to traverse the distance between the bottom edge of the task and receivers	[cm]
544	I_0	Nominal radiation	$[W.m^{-2}]$
545	I	Projection of the half-width of the receiver on the horizontal	[cm]
546	I_{1_N}	Projection of the half-width of the *spot* on the horizontal according to each mirror N	[cm]
548	K_N	Projection of the half-width of each N mirror on the horizontal	[cm]
549	L_{1_N}	Actual length of the mirror arriving on the absorber	[cm]
550	l_{a_N}	Width of the *spot* on the receiver N	[cm]
551	L_{abs}	Absorber length	[cm]
552	l_{abs}	Absorber width	[cm]
553	L_{glass}	Glass length	[cm]
554	l_{glass}	Glass width	[cm]
555	l_{mirror}	Width of mirrors	[cm]
556	$L_{receiver}$	Receiver length	[cm]
557	$l_{receiver}$	Receiver width	[cm]

M_N	Projection of the half-width of each mirror N on the vertical	[cm]
N	Number of the mirrors, the lowest mirror corresponds to the number 1 and therefore the highest one corresponds to the number 16	[ ]
P_{1_N}	power at a given moment for each mirror N	[W]
$S_{abs_{tot}}$	Total area of absorbers	$[m^2]$
S_{abs}	Surface of an absorber	$[m^2]$
$S_{mirror_{tot}}$	Total area of mirrors	$[m^2]$
S_{mirror}	surface of a mirror	$[m^2]$
T_{1_N}	Intermediate registration time (third and fourth case with first condition) according to each mirror N	[s]
T_{2_N}	Intermediate registration time (third and fourth cases with second condition) according to each mirror N	[s]
T_{N_s}	Resetting time, according to each mirror N	[s]
T_N	Exit time, according to each mirror N	[s]
X	Distance between each mirror	[cm]

Glossary

CHP Combined Heat and Power.

CPVT Concentrated PhotoVoltaic Thermal.

DER Distributed Energy Resources.

DG Distributed Generation.

DHW Domestic Hot Water.

HEATS Hybrid Electric And Thermal Solar.

LFR Linear Fresnel Reflector.

MPPT Maximum Power Point Tracking.

PVT PhotoVoltaic-Thermal.

RES Renewable Energy Sources.

SRLO Système Réfléchissant à Lames Orientables (Orientable Blades Reflective System).

References

[1] K. Darrow, R. Tidball, J. Wang, A. Hampson, Catalog of CHP Technologies, Tech. rep., U.S. Environmental Protection Agency (Sep. 2017).

[2] S. S. Joshi, A. S. Dhoble, Photovoltaic -Thermal systems (PVT): Technology review and future trends, Renewable and Sustainable Energy Reviews 92 (2018) 848–882 (Sep. 2018). doi:10.1016/j.rser.2018.04.067.

[3] L. A. Weinstein, K. McEnaney, E. Strobach, S. Yang, B. Bhatia, L. Zhao, Y. Huang, J. Loomis, F. Cao, S. V. Boriskina, Z. Ren, E. N. Wang, G. Chen, A Hybrid Electric and Thermal Solar Receiver, Joule 2 (5) (2018) 962–975 (May 2018). doi:10.1016/j.joule.2018.02.009.

[4] M. Li, X. Ji, G. L. Li, Z. M. Yang, S. X. Wei, L. L. Wang, Performance investigation and optimization of the Trough Concentrating Photovoltaic/Thermal system, Solar Energy 85 (5) (2011) 1028–1034 (May 2011). doi:10.1016/j.solener.2011.02.020.

[5] R. Daneshazarian, E. Cuce, P. M. Cuce, F. Sher, Concentrating photovoltaic thermal (CPVT) collectors and systems: Theory, performance assessment and applications, Renewable and Sustainable Energy Reviews 81 (2018) 473–492 (Jan. 2018).

[6] G. Peri, R. Masse, J. Tantardini, Solar concentration system medium temperature heliothermal using the concentration of a reflective structure to orientable blades, Mediterranean Cooperation on Solar Energy (1980).

[7] J. Chaves, M. Collares-Pereira, Etendue-matched two-stage concentrators with multiple receivers, Solar Energy 84 (2) (2010) 196–207 (Feb. 2010).

[8] P. L. Singh, R. M. Sarviya, J. L. Bhagoria, Thermal performance of linear Fresnel reflecting solar concentrator with trapezoidal cavity absorbers, Applied Energy 87 (2) (2010) 541–550 (2010).

[9] D. Beekley, G. Mather, Analysis and experimental tests of a high-performance evacuated tubular collector, Tech. rep. (1975).

[10] R. Bruno, W. Herman, H. Horster, R. Kersten, F. Mahdjuri, High efficiency solar collectors, ISES International Solar Energy Society (1975).

[11] R. Pasquetti, Numerical determination of point concentration distribution at the focus of faceted concentrators, Journal of Physics 19 (6) (1984).

[12] R. Pasquetti, G. Peri, A. Louche, A new approach for designing a solar concentrating system, Journal of Physics (1987).

[13] J. Canaletti, Study and design of the enslavement of a solar radiation concentration device (1990).